[9]The formation of transient gratings by optical interference and their detection by light scattering is well known. Previously, however, the gratings have been found to arise during excitation and to exhibit monotonic decay thereafter. See D. W. Phillion, D. J. Kuizenga, and A. E. Siegman, Appl. Phys. Lett. 27, 85 (1975), and references therein.

[10]J. C. Bergquist, S. A. Lee, and J. L. Hall, Phys. Rev. Lett. 38, 159 (1977); V. P. Chebotayev, Appl. Phys. 15, 219 (1978).

Radial Transport in ELMO Bumpy Torus with Constant Edge Neutral Flux

E. F. Jaeger and C. L. Hedrick
Oak Ridge National Laboratory, Oak Ridge, Tennessee 37830

and

W. B. Ard
McDonnell-Douglas Research Laboratories, St. Louis, Missouri 63166

(Received 18 June 1979)

One-dimensional radial transport equations for the ELMO bumpy torus are solved numerically assuming a constant flux of cold neutrals at the plasma edge. With this boundary condition, thermal stability of numerical solutions is achieved, for the first time, in the collisionless electron regime using a fully classical transport model. Results show a parametric dependence on edge neutral pressure in the collisionless regime which is similar to that observed in experiments.

Recently, one-dimensional (1D) radial transport calculations[1,2] for the ELMO bumpy torus (EBT)[3] have assumed a variable flux of cold neutrals at the plasma edge determined by instantaneous reflux of toroidal plasma particles from the wall. This leads to thermally unstable numerical solutions[2] in the collisionless electron regime where, by contrast, experiments operate stably.[3] In this paper we apply an alternative boundary condition that assumes a constant flux of cold neutrals at the plasma edge independent of toroidal plasma parameters. Such a boundary condition is appropriate if reflux from the wall occurs on a time scale that is slow compared with the energy containment time. Experiments[3] indicate that a time on the order of tens of minutes is required for the plasma to reach equilibrium with the wall. Once equilibrium is reached, pumping is balanced by a slight gas feed of $\sim 3\times10^{-2}$ Torr liter/s. This feed rate is small compared to the flux of neutrals required to sustain the plasma that is ~ 1 Torr liter/s in the present calculations. The source of these neutrals is assumed to be wall reflux.[3]

The 1D radial transport equations for EBT incorporating a self-consistent radial electric field have been discussed elsewhere.[1,2,4] The present calculations are based on a numerical solution to these equations, assuming approximate neoclassical transport coefficients that include lowest-order effects of velocity-space regions where poloidal drift frequencies are small.[2,5] For particles that experience cancellation of electric and magnetic drifts in the bulk of the velocity-space distribution (ions in EBT), the flux is dominated by slowly orbiting particles on noncircular drift orbits. In the moderate collisionality (plateau) regime, this gives transport coefficients independent of collision frequency.[2,5] Specifically, the plateau result of Eq. (14) (Ref. 2) is used for ions. For particles that do not experience such a bulk cancellation of drifts (electrons in EBT), the flux is dominated by particles with large poloidal drift frequencies and nearly circular orbits. For convenience, the large-electric-field result of Kovrizknykh[6] is used for electrons.

Numerical transport solutions in Ref. 2 assume the flux of cold neutrals at the plasma edge to be determined by the toroidal plasma through instantaneous reflux of plasma particles at the wall. In this approximation the total number of plasma particles remains constant in time. In the collisionless regime, energy containment time increases with electron temperature, and for a constant total number of particles, there is a net positive feedback in the numerical calculations in Ref. 2, causing lifetime and temperature to become arbitrarily large. Steady-state solutions exist only if the temperature dependence of the energy lifetime is modified artificially at low collisionalities.[2]

In contrast, calculations in this Letter assume

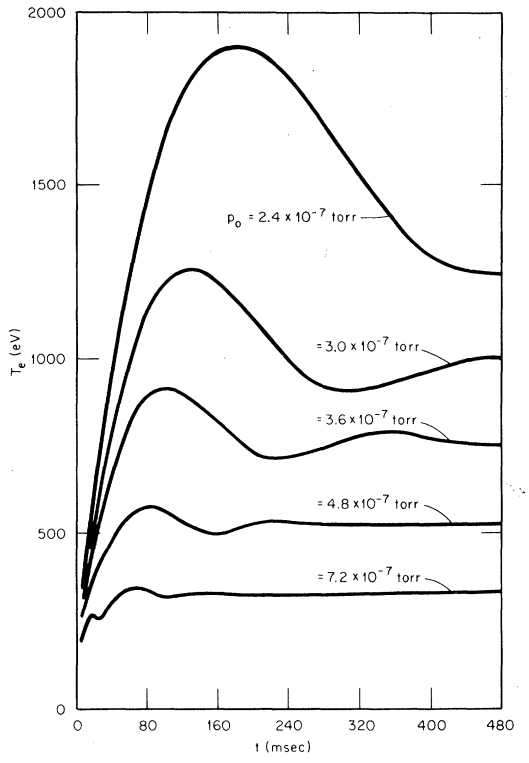

FIG. 1. Transient behavior of the axial electron temperature showing the approach to steady state for p_μ = 6 kW and variable edge neutral pressure p_0.

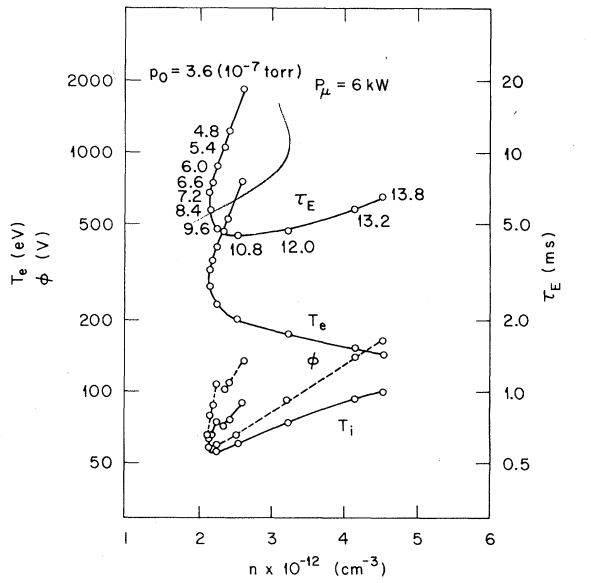

FIG. 2. T_e, T_i, φ, and τ_E vs n for steady-state plasmas with p_μ = 6 kW and varying edge neutral pressure p_0; T_e, T_i, and n are evaluated on axis. Open circles represent steady-state numerical solutions.

the flux of cold neutrals at the plasma edge to be fixed and therefore independent of toroidal plasma conditions. As the temperature and lifetime increase, so does the total number of particles, thus reducing the power deposited per particle. This provides a negative-feedback mechanism that limits thermal excursion in the numerical results and allows steady-state solutions without requiring a modification in the scaling of confinement time with temperature.

For low edge neutral pressure p_0, the negative feedback through density overcompensates for the increased lifetime and produces a damped oscillation in density and temperature. This oscillation is evident in the numerical calculations of Fig. 1, which show transient solutions for the axial electron temperature T_e when 6 kW of microwave power is applied to the toroidal plasma electrons and no power is applied directly to the ions. A time-independent, spatially uniform power-deposition profile is assumed. Results shown are for standard EBT parameters[2] (24 mirror sectors, plasma radius a = 10 cm, major radius R_T = 150 cm, bounce-averaged magnetic field on axis $B_0 \sim 6.4$ kG, cold-neutral energy $E_0 \sim 0.5$ eV, and electron-ring beta $\beta_a \sim 37\%$). At the edge $r = a$, plasma density and temperature are fixed at $n = 3 \times 10^{10}$ cm^{-3}, and $T_e = T_i = 13.5$ eV. For fixed microwave power P_μ, Fig. 1 shows that decreasing the edge neutral pressure leads to larger amplitude oscillations, smaller damping rates, and, hence, longer times to relax to steady state.

Figure 2 shows the corresponding steady-state values of electron temperature T_e, ion temperature T_i, energy confinement time τ_E, and ambipolar-potential-well depth φ vs plasma density n. T_e, T_i, and n are evaluated on axis. In all cases the shape of the potential is such as to produce a negative or radially inward-pointing electric field.[4] Edge neutral pressure is varied as a parameter along the curves. A slight discontinuity in the T_i and φ curves occurs when a cancellation of poloidal drifts becomes possible for thermal ions at some radius within the plasma.

Two distinct collisionality regimes are evident in Fig. 2. In the collisional regime, τ_E varies at $T_e^{-7/2}$ and edge neutral pressures are large. In the collisionless regime, τ_E varies as $T_e^{3/2}$ and edge neutral pressures are low. Results in Fig. 2 are reminiscent of early zero-dimensional (0D) power balances[7] for EBT that assumed *ad hoc* electric fields with $e\varphi/kT$ constant. If plateau transport for ions is included in a similar simplified point model with constant edge neutral density, the steady-state results in Fig. 2 are ap-

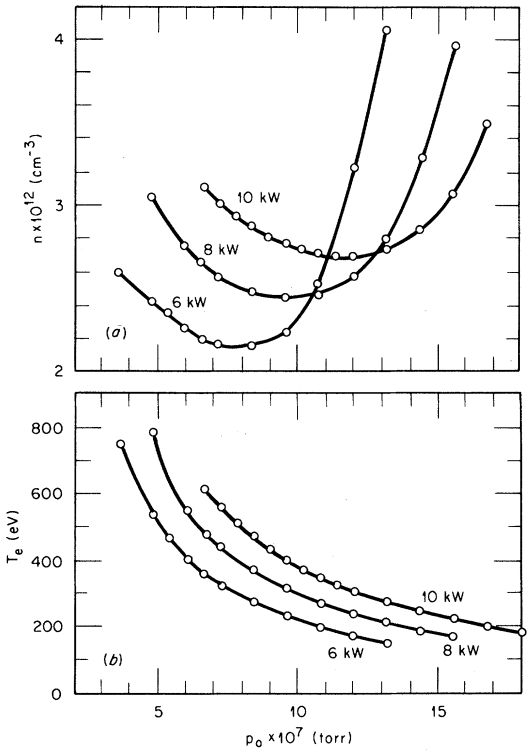

FIG. 3. Plasma density (a) and electron temperature, (b) vs edge neutral pressure p_0 for $p_\mu = 6$, 8, and 10 kW. Open circles represent steady-state numerical solutions.

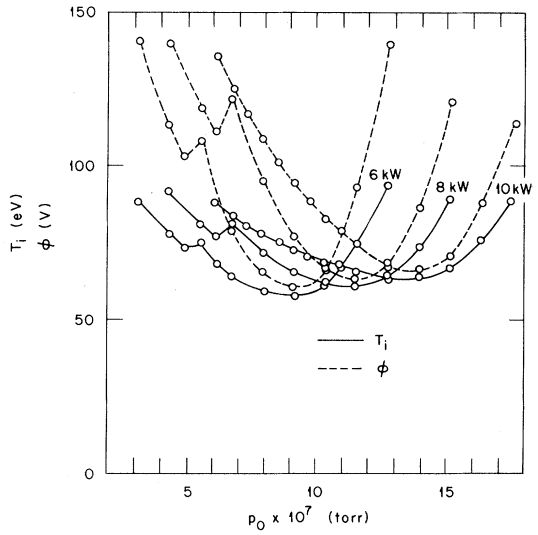

FIG. 4. Ion temperature (solid) and potential well depth (dashed) vs edge neutral pressure for p_μ = 6, 8, and 10 kW. Open circles represent steady-state numerical solutions.

proximately reproduced. Furthermore, a linear stability analysis predicts thermal stability for all collisionalities with decreasing damping rates in the collisionless regime. Alternatively, if constant plasma density is assumed (0D equivalent of instantaneous reflux), then collisionless solutions become thermally unstable while collisional solutions remain stable. The stability boundary occurs at the point of minimum plasma density.

Experimental results are often plotted versus ambient neutral pressure as given by ion gauges.[3] For comparison with such data, we replot the numerical results of Fig. 2 as a function of $p_0 = n_0 k T_0$, where n_0 is the density of cold neutrals at the plasma edge and $kT_0 \equiv E_0 \sim 0.5$ eV. Note that p_0 is similar but not equal to the ion-gauge pressure. Results shown in Figs. 3 and 4 include additional microwave powers $P_\mu = 8$ and 10 kW. Open circles represent thermally stable, steady-state numerical solutions to the 1D transport equations. In the collisionless regime (low neutral pressure), the parametric dependence on edge neutral pressure is similar to that observed in experiments[3]; i.e., density, temperature, and potential all increase with decreasing neutral pressure (see Figs. 30 and 32 in Ref. 3). Experiments apparently do not observe the collisional scaling shown at high neutral pressures in Figs. 3 and 4 because electron-ring β is not sufficient to stabilize the toroidal plasma in this regime.

Calculations reported here represent the first thermally stable, fully classical 1D transport solutions for EBT in the regime of the experiment, i.e., collisionless electrons with negative electric fields. It has been shown that in this regime, density, temperature, and potential all increase with decreasing neutral pressure. Also, as the collisionless regime is penetrated, damping rates decrease rapidly, making the plasma more susceptible to small perturbations. However, present theory does not predict a minimum collisionality below which perturbations grow unstably (M mode[3]). This may require additional physics assumptions with regard to interaction of the toroidal core plasma and the hot-electron rings.

The authors wish to thank H. C. Howe and J. T. Hogan for helpful discussions. This research was sponsored by the Office of Fusion Energy, U.S. Department of Energy, under Contract No. W-7405-eng-26 with the Union Carbide Corporation.

[1]E. F. Jaeger and C. L. Hedrick, Nucl. Fusion 19, 443 (1979).

[2]E. F. Jaeger *et al.*, Oak Ridge National Laboratory

Report No. ORNL/TM-6806, 1979 (unpublished).
[3]R. A. Dandl *et al.*, Oak Ridge National Laboratory Report No. ORNL/TM-6457, 1978 (to be published).
[4]E. F. Jaeger *et al.*, Phys. Rev. Lett. 40, 866 (1978).
[5]R. D. Hazeltine *et al.*, Science Applications, Inc., Report No. SAI-02379-664LJ, 1979 (to be published).
[6]L. M. Kovrizhnykh, Zh. Eksp. Teor. Fiz. 56, 877 (1969) [Sov. Phys. JETP 29, 475 (1969)].
[7]R. A. Dandl *et al.*, Oak Ridge National Laboratory Report No. ORNL/TM-4941, 1975 (unpublished).

Spontaneous, Three-Dimensional, Constant-Energy Implosion of Magnetic Mirror Fields

Paul M. Bellan
California Institute of Technology, Pasadena, California 91125
(Received 8 June 1979)

Experimental and theoretical results are presented concerning a method for providing three-dimensional spontaneous implosion of a magnetic mirror field. This is achieved by making the mirror field a propagating macroscopic wave in a medium for which the wave velocity is a slowly changing function of position. Slowing down of the magnetic mirror wave causes WKB steepening and shortening—i.e., three-dimensional field compression—in a manner wherein the total magnetic field energy stays constant.

Rapidly increasing the current in the field coils of a magnetic mirror is effective for both heating mirror-confined particles and increasing their density.[1] However, this compression technique is inefficient, because magnetic energy, W_B, scales as B^2, while particle energy, $T_\perp$, scales only as B. Hence, more energy goes into creating new magnetic field lines than into heating particles. The imploding liner[2] partially avoids this problem by decreasing (in a flux-conserving manner) the field cross-sectional area as B increases so that W_B will scale as B. Unfortunately this method involves difficult engineering problems if a repetitive system is wanted, as for a fusion reactor.

I present here experimental and theoretical results on an entirely new method of adiabatic compression which does not involve liners and which provides a three-dimensional compression at essentially *constant* magnetic field energy. This is achieved by compressing the magnetic field volume in all three dimensions so that as B increases, $W_B = B^2V/2\mu_0$ stays constant. The three-dimensional nature of this compression gives both three-dimensional heating and a greater density increase than two-dimensional compression. Because only passive components are used and because the compression ratio is determined solely by the system geometry (and not by the energy input), the effective result is a spontaneously imploding, magnetic mirror.

In this scheme a moving magnetic mirror is created by arranging for the mirror field to be a propagating distrubance in some medium. It becomes, in effect, a macroscopic wave, carrying particles trapped in its trough. WKB theory states that the characteristic axial length and intensity of such a propagating disturbance can change if the characteristic wave velocity of the medium is a slowly varying function of position in the medium. In particular, in regions where the wave velocity decreases, the magnetic-mirror wave shortens and steepens in a manner wherein its total energy stays constant. When this wave steepening occurs, adiabatic compression of particles trapped by the mirror will result. The particles are heated in the perpendicular direction ($T_\perp \propto B$), in the parallel direction ($T_\parallel \propto \lambda^{-2}$, where λ is the axial extent of the mirror field), and are compressed in three dimensions ($n \propto B/\lambda$). The compression occurs at constant (except for diamagnetic effects) W_B, and the compression ratio depends only on the geometric properties of the medium, and not on the energy input.

A practical realization of the above field compressor has been constructed. In this device (c.f. Fig. 1) coils comprising a long solenoid are connected to capacitors, each having capacitance C, so as to form a variation on a lumped-element delay line.[3] Pulses injected onto the delay line propagate along it with a characteristic velocity determined by the inductances, capacitances, and intercoil spacings. In particular, a double-humped[4] pulse of the type shown in Fig. 1(a) also propagates down the delay line at the characteristic velocity. Associated with this current pulse is an axially propagating double-humped solenoidal magnetic field—i.e., the axially propagating magnetic mirror. This solenoid delay line is thus the

